Universal behavior of ^{4}He films as a function of thickness near the Kosterlitz-Thouless transition

D. Finotello,* Y. Y. Yu,† and F. M. Gasparini
Department of Physics and Astronomy, State University of New York at Buffalo, Buffalo, New York 14260
(Received 10 August 1989; revised manuscript received 12 February 1990)

We report measurements of the convective conductance of ^{4}He films near the Kosterlitz-Thouless transition. Data for 14 films are analyzed over a range of critical temperatures from 1.28 to 2.16 K, and thicknesses 11.7 to 156 Å. We obtain good agreement using two different methods of analysis with the predicted behavior of the dynamic theory. The exponential divergence is observed up to six decades in conductance and one decade in reduced temperature. We find that the parameter b, which determines the sharpness of the divergence, and also the cusp in the superfluid density increases with film thickness. This is consistent with the growth of the three-dimensional correlation length. We find also that the ratio of diffusion constant to the square of the vortex core radius, D/a^2, is a decreasing function of film thickness. We compare this with measurements in which D is obtained directly. We also report measurements of the nonlinear dependence of the conductance below the transition. These are shown to be consistent with measurements above the transition.

I. INTRODUCTION

The superfluid properties of ^{4}He films have been studied for many years and continue to be a source of new and interesting physics. At the simplest, films may be looked at as a two-dimensional (2D) analogue of bulk helium. Thus, at low temperatures, films may be described in terms of elementary excitations which mirror in a lower dimension the excitations of the bulk. Films, however, are much more than this because of the additional variables associated with the liquid-substrate and liquid-gas (or vacuum) interfaces. Interesting phenomena are associated with these interfaces for both ^{4}He and ^{3}He, and, as well, for isotopic mixtures.

Near the superfluid transition, in particular, films of ^{4}He differ in a fundamental way from bulk helium in the sense that they belong to a different universality class, a 2D XY system. As such, their critical behavior is quite different and distinct from that of bulk helium. The heat capacity, which in 3D has a nearly logarithmic singularity,[1] is expected to be perfectly regular in 2D.[2–4] The superfluid density, which in 3D vanishes with a nearly $\frac{2}{3}$ power law,[5] has a discontinuity at T_c in 2D.[6,7] The thermal conduction, which in 3D has a nearly $\frac{1}{3}$ power-law divergence[8] above the transition, is exponentially divergent in 2D.[9–13]

The critical behavior in 3D is well understood. Measurements at present can be done as close as $t \equiv |T/T_\lambda - 1| = 10^{-7} - 10^{-8}$ of the transition and are approaching a level where, with reasonable samples, substantial gravitational rounding can take place. Studies of bulk helium have yielded very precise checks on theories of critical behavior and scaling relations.[14] In particular, the concept of universality has been checked in a variety of experiments both along the λ line in the pressure-temperature plane and in the temperature–^{3}He-concentration plane.

By comparison with bulk helium, the critical behavior of films at the transition is much less well understood, and certainly not measured with a precision analogous to the bulk. The reason is that measurements with films are more difficult. One can run into difficulties associated with substrate quality, finite-velocity and frequency effects, film uniformity, and ultimately size effects associated with an exponentially divergent correlation length. Films, on the other hand, are very interesting because they are a realization of a different universality class which can be obtained over an arbitrary range of thickness provided one has the temperature resolution. More specifically, a film will undergo a 2D transition after, or when, the 3D correlation length becomes comparable to the film thickness. This "event" takes place progressively closer to the bulk transition T_λ as $d \to \infty$. The point is, however, that if one looks at d as simply a variable (analogous to the pressure for 3D) which shifts T_c, the 2D critical temperature, then the universal behavior can be studied over an infinite range of d. There are obviously practical limitations to this. One of them is the fact that as d increases the 2D region becomes very narrow in temperature and is mixed strongly by the "background" behavior associated with finite-size 3D critical behavior. This latter is itself of substantial interest in testing ideas of finite-size scaling.[15]

In this paper, we report measurements of thermal conductivity of films near the superfluid transition over a thickness range from $d = 11.7$ to 156 Å. One may view this work as a study of the universal character of the transition as a function of d. It is thus analogous to studies of the 3D transition as a function of pressure. Measurements of thermal conductivity have been reported previously, but not to explore the d-dependence as in our work. Shorter reports on our work have been published previously.[13,16] Another publication from our work addressing issues of finite-size scaling has already appeared.[4] Our work with mixture films will be published separately.

Below we discuss the theoretical background behind our measurements. This is followed by a discussion of ex-

perimental details, data and data analysis. Before a summary and conclusion, we compare our work with relevant earlier results.

II. THERMAL CONDUCTION IN ^{4}He FILMS

The transport of heat in a helium film near the superfluid transition is a convective process: liquid flows toward a hot surface at which it evaporates. Gas then flows toward the cold surface where it completes the cycle by giving up its latent hat. Such a process is obviously realizable only when the vapor pressure of the gas is sufficiently high. Practically, this means temperatures above ~ 1.1 K and superfluid films greater than about an atomic layer. This convective process is much more analogous to thermal counterflow in bulk helium below T_λ than to the diffusive thermal conductance measured above T_λ.

The superfluid phase of helium films is understood within the Kosterlitz-Thouless (KT) theory[2] as consisting of a background superfluid density ρ_{s0} which is stabilized and modified by the presence of pairs of vortices with opposite circulation. At the transition, vortices paired at the largest separation begin to break up due to thermal fluctuations. This process continues as one moves above the transition until pairs at the smallest scale are no longer bound. The static superfluid density at the transition should jump discontinuously to zero.[17] This, in fact, has never been measured since all experiments to measure ρ_s involve dynamic processes which render ρ_s continuous through the transition. Theories of the dynamic aspects of the KT transition in helium films have been developed by many authors.[18–22] In particular it was pointed out by Ambegaokar, Halperin, Nelson, and Siggia (AHNS)[18] that the convective conduction of a film near the transition should be inversely proportional to the density of free vortices, hence, the square of the 2D correlation length. Expressions for the thermal conduction for a geometry appropriate to our experiment were derived in greater detail by Teitel.[23]

The situation considered by Teitel is that of a chamber consisting of two parallel surfaces linking two plates (see Fig. 3 in Ref. 23). One is maintained at a temperature T_0 while the other is heated above this by an amount ΔT. A film of helium formed on the walls of this chamber moves in response to the ΔT while evaporating atoms reflux in the opposite direction. This convective process is described by the time-independent hydrodynamic equations of third sound. Two modifications are necessary: one is the inclusion of a dissipative term due to vortex motion in the equation of the superfluid; the other is the replacing of ρ_s which is zero above T_c by ρ_{s0}, the background superfluid density in the absence of vortices. One has

$$\hat{z}\times\mathbf{J}_v+\nabla\mu_f=0 , \tag{1}$$

where $\hat{z}$ is the direction perpendicular to the film, $\mathbf{J}_v$ is the vortex flux, μ_f is the film's chemical potential. No additional equations are necessary if one assumes that there is no net mass flow either along the direction of the film or perpendicular to it. One also has to assume that substrate and film are at thermal equilibrium. All these are good assumptions for the geometry of our experiment. See, however, Hedge *et al.*[24] for an experimental geometry where the flux of atoms perpendicular to the film cannot be ignored.

To cast Eq. (1) in terms of measurable quantities, we note that we must have for the gas and film $\mu_g=\mu_f$. Thus, $\nabla\mu_f$ can be calculated from $\nabla\mu_g=\rho_g\nabla T-\rho_g^{-1}\nabla P$. The pressure can be eliminated by noting that for viscous flow between two parallel surfaces at a distance d apart, $\mathbf{v}_g=-(d^2/12\eta)\nabla P$, where η is the viscosity. For the first term in Eq. (1), Teitel follows AHNS and replaces this term by an average over the whole surface over which the film flows. This gives

$$\langle\hat{z}\times\mathbf{J}_v\rangle_{\text{free}}=(2\pi\hbar/m)^2(D/k_BT)\rho_{s0}n_f\mathbf{v}_f , \tag{2}$$

where D is the diffusion constant and n_f is the number of free vortices per unit area. To arrive at 2 it is assumed that an equal number of vortices of opposite circulation are present. Putting these results together one obtains,

$$\rho_{s0}v_s\left[\left[\frac{2\pi\hbar}{m}\right]^2\frac{D}{k_BT}n_f+\frac{24\eta}{\rho_g^2d^3}\right]=S_g\Delta T . \tag{3}$$

Or, relating the power adsorbed to the latent heat $\mathcal{L}$ transported by the gas, $Q=\mathcal{L}W\rho_{s0}v_s$, we have

$$Q=\frac{\mathcal{L}^2(W/L)}{(2\pi\hbar/m)^2(D/k_B)n_f+24\eta T/\rho_g^2d^3}\Delta T , \tag{4}$$

where we set $\mathcal{L}=TS_g$ and W, L, are, respectively, the perimeter over which the film flows and the distance across which ΔT appears.

There are two further modifications necessary in Eq. (4). One must allow for the parallel conduction associated with the structural material of the cell, the *diffusive* conduction of the gas itself and, in principle, of the film as well. We can lump all of this together into a term we call K_b, for the small background conductance. The other addition is to recognize that to get heat in and out of the helium one must overcome a boundary resistance which is in series with the convective film mechanisms. See below. In summary, we may write that the measured thermal conductance K_m is given by

$$K_m\equiv\frac{Q}{\Delta T}=K_b+\left[\frac{1}{K_f}+\frac{1}{K_g}+\frac{1}{K_K}\right]^{-1} , \tag{5}$$

where we have separated the film flow and gas refluxing terms as K_f and K_g. In a properly designed experiment one wants $K_b\ll K_f\ll K_g\sim K_K$. In this limit, one has $K_m\simeq K_f$. Consequently, see Eq. (4), K_m yields directly the density of free vortices. According to AHNS, n_f can be assumed to be proportional to the square of the inverse of the 2D correlation length above T_c,

$$n_f\sim\xi_+^{-2}=a^{-2}\exp(-4\pi t^{-1/2}/b) , \tag{6}$$

where $t\equiv(T/T_c-1)$ and b is a constant which may depend on the film thickness and is not a universal number for different 2D XY systems. The constant a is the vortex core parameter which will itself depend on the film thickness. With Eq. (6), we may write K_f as

$$K_f = F\frac{\mathcal{L}^2(W/L)}{(2\pi\hbar/m)^2(D/a^2)k_B}\exp(4\pi t^{-1/2}/b)\ , \qquad (7)$$

where F is a proportionality constant of order unity. This equation shows the very strong exponential temperature dependence which K_f is expected to have near T_c. Experimentally the divergence is limited by K_g or K_K; and, away from T_c, one cannot obtain K_f once it falls substantially below K_b.

There is one important assumption in writing Eq. (6) and hence (7). All the free vortices are attributed to the "natural" mechanism of vortex unbinding due to thermal fluctuations. In practice, since one must drive the film at a nonzero velocity to obtain a measureable ΔT, one will always create additional free vertices. Below the transition, where $n_f=0$, it is impossible not to perturb the system via a small flow. Above T_c, however, one can extrapolate the measurement to $Q=0$, i.e., $v_{s=0}$, or work at sufficiently low velocities that thermally activated vortices always dominate. In practice this procedure becomes more difficult as one approaches very close to T_c.

Below T_c, one still retains the relationship $K_f \propto n_f^{-1}$, but one must calculate an equilibrium value for n_f as the result of vortex unbinding due to finite velocities. This has been done by a number of authors.[18,19,22] There is a possibility, as well, that due to film imperfections vortices might be pinned at special sites and freed upon imposition of a velocity field.[21,22] The depairing and depinning mechanisms yield quite different dependence of n_f on v_s. To obtain the equilibrium value for n_f, one must consider vortex recombination rates as well as creation, annihilation at film boundaries. For temperatures not too close to T_c, AHNS derive for a depairing mechanism

$$n_f \sim \frac{bt^{1/2}}{a^2}\left[\frac{a}{r_c}\right]^{2+\frac{b}{2}t^{1/2}}\ , \qquad (8)$$

where $r_c \sim v_s^{-1}$, is the critical distance at which vortex pairs unbind due to the velocity field. The restriction of not being too close to T_c comes from the requirement that r_c must be much larger than ξ_-. This latter is given by $\ln(\xi_-/a)=(bt^{1/2})^{-1}$, a length determined by the renormalized dielectric constant below T_c.[18]

We note now that since $v_s \propto Q$, we have due to depairing

$$K_f \sim Q^{-(1/2)(4+bt^{1/2})}\ . \qquad (9)$$

This equation for $T<T_c$ can be tested experimentally and allows one to obtain *independently* a value of b which can be compared to the value obtained via Eq. (7) for K_f at $T>T_c$. Note, as remarked before, that Eq. (9) would not be appropriate to an experimental situation where there would be convective gas flow in a direction perpendicular to the film.[24]

III. APPARATUS AND PROCEDURE

The requirements to make a measurement of thermal conductivity of helium films near T_c are as follows. An experimental cell is needed which contributes a small background conductance and allows for the formation of helium films over as wide a range of thickness as possible. Long-term temperature stability is required as well as high resolution to measure small temperature differences at very low-power inputs. The film thickness must remain constant, or very nearly so, as the temperature is varied. We discuss below how these requirements were met in two experimental cells we used.

A. Cells

Our first experimental cell is shown in Fig. 1.[25] To minimize the conductance of the structural materials of the cell, the substrate for the films were chosen to be a combination of Mylar and Kapton.[26] A strip of Mylar, 300 cm long, 2.5 cm wide and 2.54 μm thick was wound in a cylindrical geometry with a 100 μm paper spacer at the ends. This precaution was taken to ensure a relatively open spacing between the Mylar layers. This minimizes the viscous drag that could limit the convective heat transport and avoids capillary condensation of the film. Further, small holes were randomly punctured in the Mylar strip to aid in vapor equilibration.

The inner and outer body of the cell were made out of 50 μm Kapton sheet, type *H*. The Kapton sheet was formed into open-end cylinders and sealed along its length with 1266 epoxy. The inner cylinder had a 1.2 cm diameter, while the outer cylinder had a 2.5 cm diameter. The Mylar roll was then staged within the Kapton walls. A spacing of 1 mm existed between the first and last Mylar layers and the Kapton housing. We used a Kapton housing instead of Mylar simply because it binds better to epoxy.

The cylindrical assembly was then placed to link two goldplated oxygen-free-high-conductivity (OFHC) copper plates. A mixture of 1266 epoxy[27] and copper powder was used to bind the ends of Mylar roll and to seal the Kapton housing to the copper plates. The idea was to improve the thermal contact between the helium and the

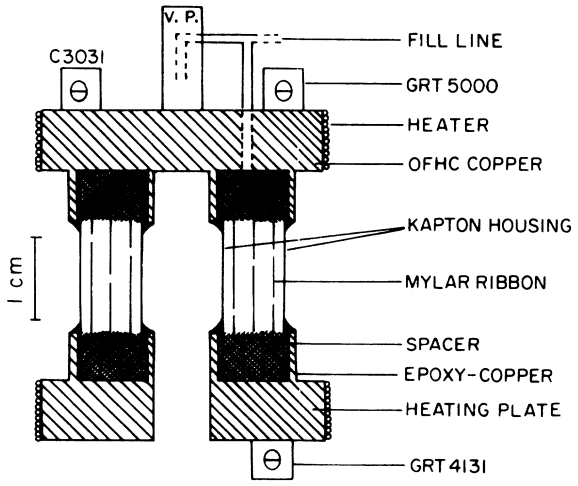

FIG. 1. Cross-sectional view of our first experimental cell. V. P. denotes the vapor pressure gauge. The symbol θ denotes two germanium, GRT, and one carbon glass thermometers.

copper plates where the temperature is actually measured.

The copper bottom plate was provided with a heater and a germanium thermometer. The top plate also had a heater and a carbon glass thermometer which was used for temperature regulation. It included also a germanium thermometer of similar characteristics to that at the bottom plate. These two fairly well-matched germanium thermometers were used to perform a differential temperature measurement. The copper top plate was also provided with a vapor pressure gauge. The pressure inside the cell was monitored via a capacitive measurement of this gauge as compared with a standard capacitor anchored at this top plate. This capacitor was based on the design of Steinberg and Ahlers.[28]

The net spacing for heat transport in this cell is 1 cm. The perimeter for film flow is 612 cm. The open volume of the cell is 7 cm^3 with a surface area of nearly 1250 cm^2. In order to minimize changes of film thickness as the temperature is changed, we had to improve on the surface to volume ratio. We did this by connecting the cell to an area reservoir consisting of Nuclepore filters.[29] This was kept isothermal to the top plate. The surface area was now 1.15×10^6 cm^2 as measured by N_2 adsorption and the surface to volume ratio 4×10^4 cm^{-1}. This arrangement, as well as the overall low-temperature configuration, is shown in Fig. 2.

The experimental cell is placed within a light shield isothermal to the regulated top plate. The total arrangement of cell and Nuclepore reservoir is weakly linked to a ^{4}He evaporator. This link was achieved through seven copper wires, 25 cm long and 0.4 mm in diameter and estimated conductance of 5×10^{-4} W/K. A second light shield provides an isothermal enclosure as shown in Fig. 2.

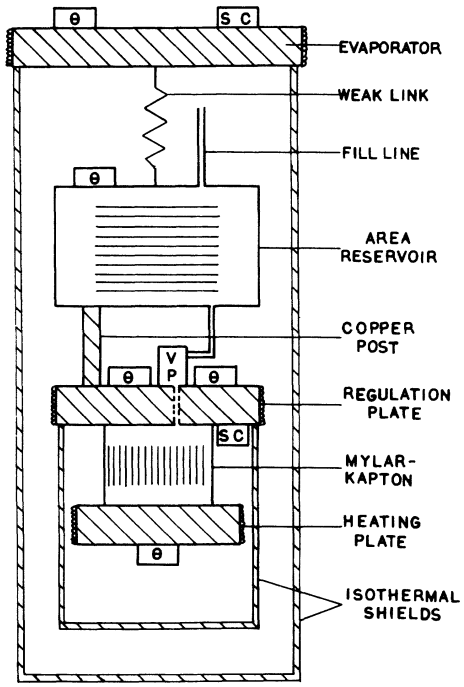

FIG. 2. Overall experimental arrangement. The experimental cell is shown schematically, a more accurate representation is given in Fig. 1.

The arrangement for the above cell is suitable for measuring films up to about 58 Å in total thickness above the Mylar substrate (56 Å for the Nuclepore). At this point capillary condensation onsets in the 2000 Å Nuclepore filters and film homogeneity is much harder to control.[30] In order to work with thicker films, we designed a second cell.[31] This is discussed in detail in Ref. 4. Films of helium are formed in this cell on a Kapton surface which is at a controlled distance from a reservoir of bulk liquid helium. The thickness of the film in equilibrium with the reservoir is dictated by the strength of the van der Waals attraction of the substrate and the gravitational potential at a given height above the reservoir. The details of how the film thickness is calculated for this cell are also given in Ref. 4. With these two cells we were able to measure films ranging in thickness from 11.7 to 156 Å, and T_c ranging from 1.28 to 2.16 K. Note that possible errors in our measurements associated with film thickness are quite different in the two experimental cells. It is thus quite important that the results from these two cells are consistent. This, in fact, was more important for the finite-size-scaling aspects of our data[4] than for what we will be discussing in this paper. Here we mostly parametrize our results in terms of T_c, which is self-determined for each film measured. The data reduction to obtain the film conductance is slightly different for these two cells. This is discussed in the Appendix, and see also below. Also, for the two cells heat was supplied in one at the bottom, and the other at the top. No instability due to gas conduction was seen in the range of powers we used.

B. Temperature control and measurement

To achieve good temperature stability at the cell, several points in the experimental arrangement shown in Fig. 2 are thermostated. First, the evaporator is either left self-regulating at its lowest temperature or electronically controlled at a temperature slightly below the cell's. This is done using a resistance bridge and proportional-integral-differential feedback to a heater. The cell filling line, which runs through a vacuum line to room temperature, is weakly linked to the evaporator and regulated typically at about 3 K. The most crucial regulation is at the top plate of the cell. This is done at the temperature at which the measurement is to be taken. This regulation could be done to better than 1 μK for most of the temperature range. The overall drifts over a 10 h period were several μK for the first cell and a factor of 3 worse for the second cell. These long-term drifts are not very important. In fact, for any given film, data were taken typically over a period of 4–6 weeks with overlapping points taken in successive days. The absolute temperature is calibrated to the T58 ^{4}He vapor pressure scale.[32] This was done through an intercomparison with a precalibrated germanium resistor. This was also checked again against the vapor pressure of ^{4}He using the low-

temperature pressure gauge at the cell. This latter was calibrated against a room-temperature gauge.

To obtain the thermal conductance one has to measure the temperature difference between the top and bottom plate of the cell upon the application of a given heat input. This was accomplished by using a differential resistance measurement between two well-matched germanium resistors at the top and bottom plates. These resistors are part of a Zair-Greenfield variation of a Kelvin double bridge.[33] In this design one uses unity gain voltage followers in the voltage arms of the bridge. This ensures that the same current passes through both resistors. Further, this bridge eliminates the output transformer and substitutes for it a differential amplifier. The balancing element in the bridge is a precision ratiotransformer. Thus, one can achieve high-temperature resolution. The temperature difference between bottom and top plate ΔT can be expressed to a very good approximation as

$$\Delta T = \frac{\delta R}{R}\left[\frac{1}{r}\frac{dr}{dT}\right]^{-1}, \tag{10}$$

where δR is the change in the ratiotransformer setting, R; and, $(1/r)(dr/dT)$ is the fractional resistance change of the bottom thermometer with temperature. Equation (8) is derived in the Appendix. If $\delta R/R$ can be resolved to 10^{-6}, then with typical germanium thermometers, ΔT can be resolved to $\sim 0.5\times 10^{-6}$.

There is an important limitation in measuring ΔT. Since the power dissipation at the bottom thermometer adds to the power used in obtaining ΔT, and since the conductance is often a nonlinear function of power, then the power dissipated must be always much smaller than the heater power used to obtain the measured ΔT. No such limitation is imposed on the regulation thermometer at the top plate of the cell.

In Fig. 3 we show an example of how our data are obtained. This is taken from a stripchart recorder where a signal proportional to the temperature difference between the top and bottom plate of the cell is monitored as a function of time. Four "steps" are shown in this figure. These correspond to incremental power inputs to the bottom plate of the cell. The conductance is the ratio of the power applied to the temperature offset. Note that for the data in this figure, this ratio is nonlinear in the power. This is because the cell temperature is below the superfluid transition of the film. Measurements such as these give the power (i.e., velocity) dependence of the film conductivity. Above the transition, but close to T_c, these measurements allow one to extrapolate the film conductivity to zero power. Well above the transition, these measurements show a strictly linear dependence of temperature offset with power. In this region a single power is needed to obtain the conductance. Note that none of our measurements are done by fixing the power and obtaining ΔT as a function of temperature. This procedure would introduce systematic errors in the data due to the power dependence of the conductance close to T_c.

The amount of time one waits at any given power depends on the relaxation times and how long one wants to integrate the noise in the temperature. Anomalous drifts or steps which may appear during the measurements shown in Fig. 4 are sometimes due to slips in the regulation. This can easily be checked by turning the heater power off and verifying that the zero-power level is reproduced. The two differential thermometers can also be read independently. Thus, one can check that all three thermometers track during a series of measurements.

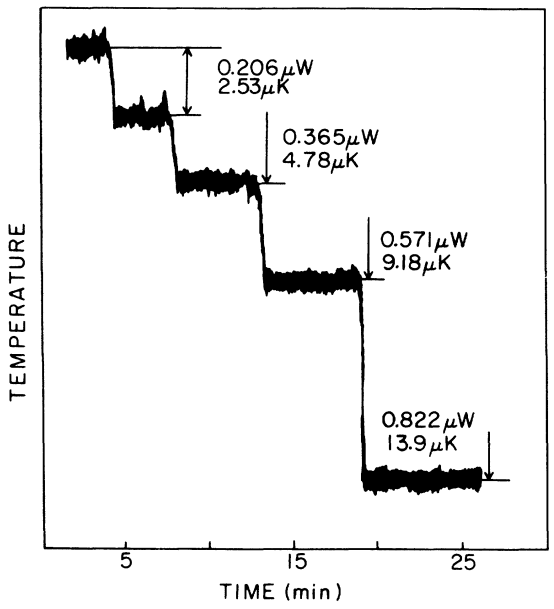

FIG. 3. Temperature offset of the differential bridge at four different powers applied to the bottom plate of the cell. The top plate of the cell is regulated at a fixed temperature below the transition.

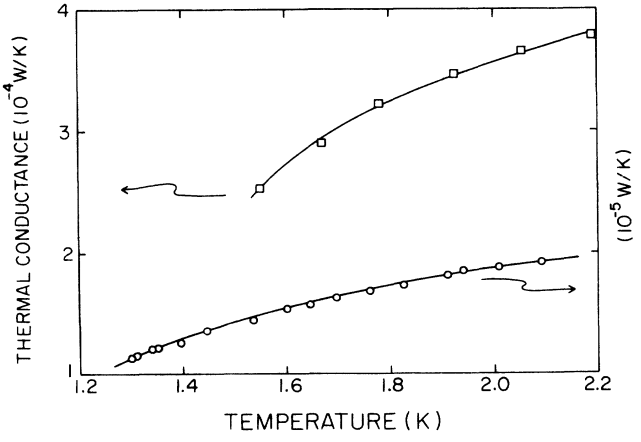

FIG. 4. Thermal conductance as a function of temperature for the two experimental cells used in our work. The top curve is for the Kapton cell, the bottom for the Mylar cell. This is the background conductance without any contribution from the helium gas.

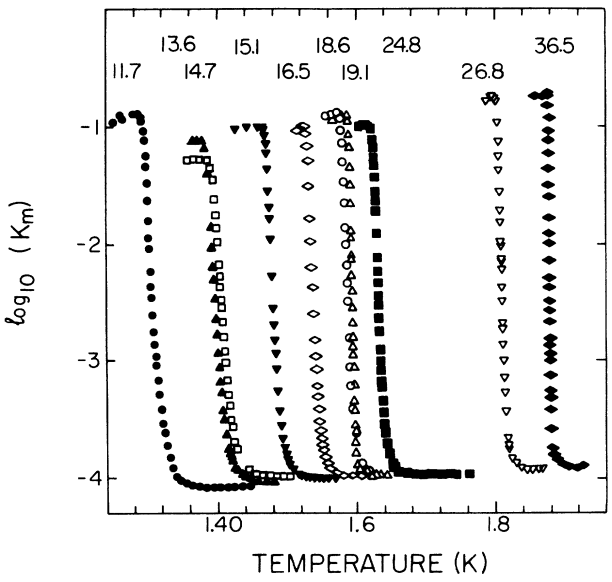

FIG. 5. The measured conductance K_m on a log scale as a function of temperature for the ten thinnest films we have measured. K_m is in WK^{-1}. The numbers refer to the film thickness in Å.

C. The pressure gauge

We use the low-temperature pressure gauge for several purposes. By knowing the pressure we can calculate the latent heat of evaporation which is needed to analyze the data [see Eq. (4) and below]. For the unsaturated films, we calculate the thickness from the amount of helium admitted to the cell and the total low-temperature surface area. This requires that we know the pressure to allow for the number of atoms in the gas phase. Further, as the temperature is changed, the film thickness will change. This can be calculated and a correction applied to the data in a self-consistent way so that it represents the conduction of a film at constant thickness. Typically for our cell the film will change by about 2% over the region in which we analyze the data. This is a small effect per se, however, since the film conductance is singular in the

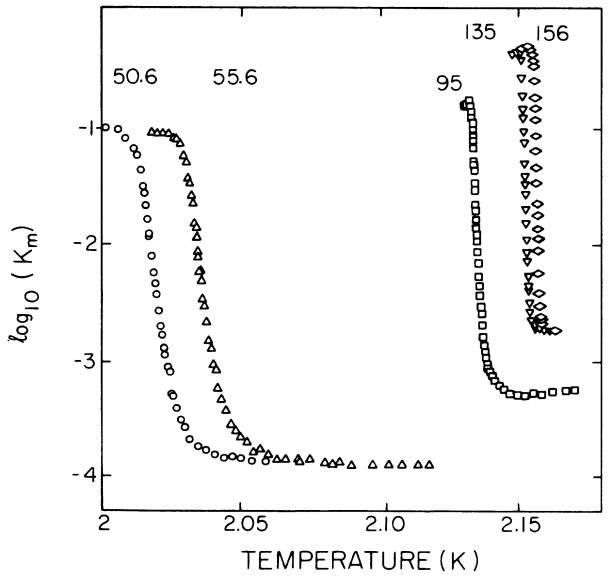

FIG. 6. The measured conductance K_m on a log scale as a function of temperature for the five thickest films. Note the expansion of the temperature scale by a factor of 4 relative to Fig. 5. The thickest three films shown are saturated films.

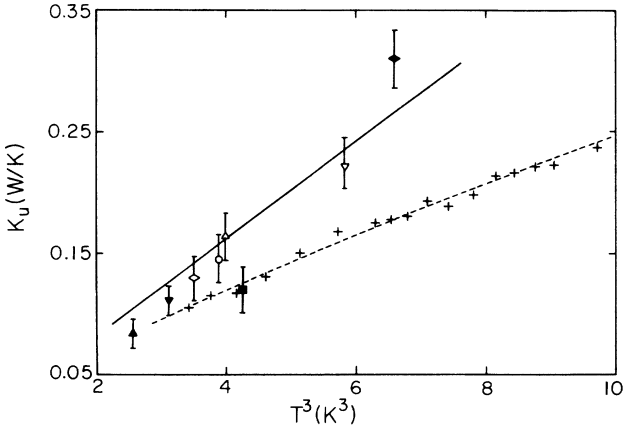

FIG. 7. Solid symbols, the highest value of measured conductance K_u for films of different thickness. Plusses, the temperature dependence of K_u for a thick film. The solid line is drawn to guide the eye. The dashed line is a least-squares power-law fit. See text.

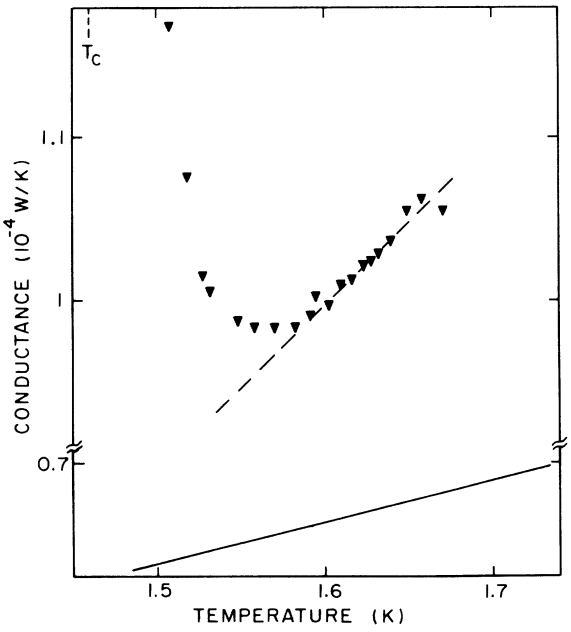

FIG. 8. The measured film conductance near its smallest value for the 15.1 Å film. The dashed line indicates a background conductance fit to the high-temperature region of the data. The solid line is the expected background on the basis of the empty cell and gas contributions.

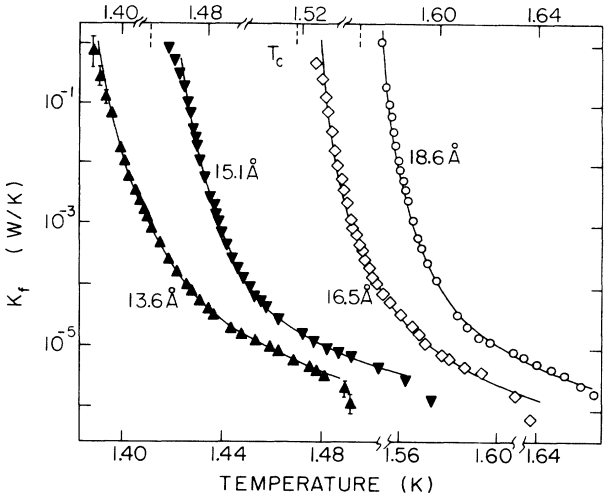

FIG. 9. Log of the film conductance K_f as function of temperature. Note that these data are on the same linear temperature scale, but there are breaks in the temperature axis. The dashed vertical lines indicate T_c. The solid lines are least-squares fit to the expected theoretical behavior.

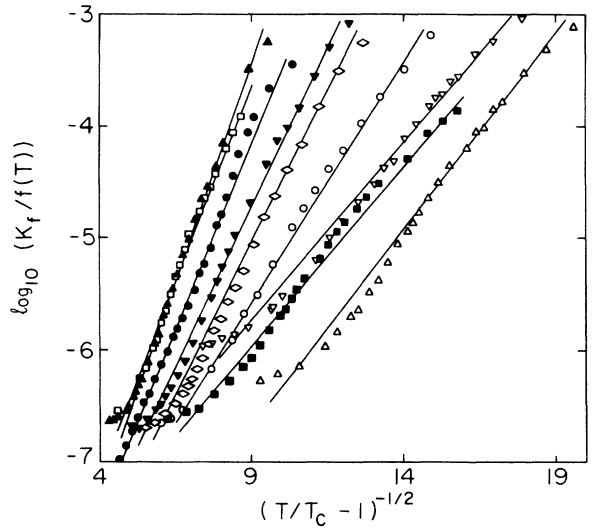

FIG. 11. Semilog plot of $K_f/f(T)$ in sec vs $t^{-1/2}$. Symbols correspond to film thickness as indicated in Fig. 5. The solid lines are least-squares fitted to the data analyzed via method two.

thickness, this must be taken into account. We do this as follows. We first assume that the thickness does not change. This gives us an initial set of parameters, D/a^2, T_c, and b, which can be used to calculate the effect of a changing thickness. This process is repeated 2–3 times until the parameters no longer change. The parameters obtained with and without this correlation will be discussed below. Further details of this analysis are given in the Appendix. This analysis is not essential for some of the trends in the conductance which we will discuss; however, it puts the data for the unsaturated films on equal footing with the unsaturated films where this analysis is *not necessary*.

The gauge itself is after the design of Greywall and Bush.[34] It consists of a capacitive transducer with one plate at the top of a diaphragm which moves subject to pressure. The capacitance between this plate and a sta-

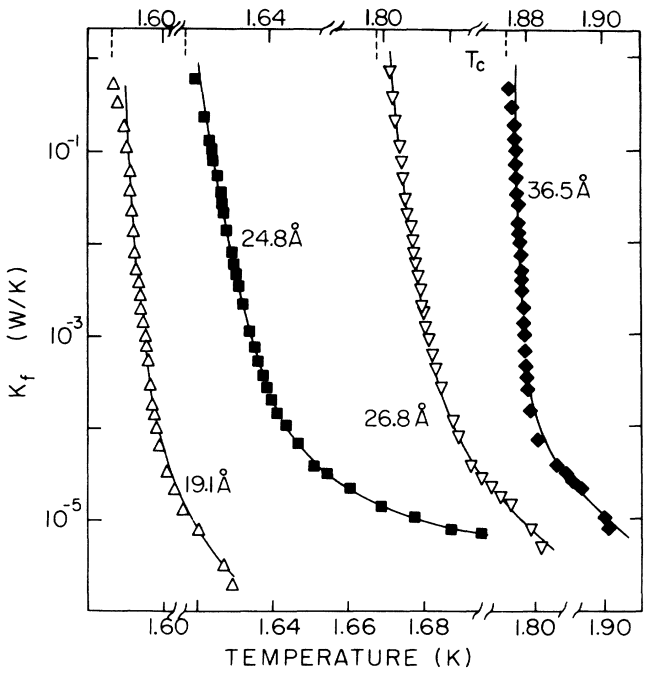

FIG. 10. Log of the film conductance K_f as function of temperature. Note that these data are on the same linear temperature scale, but there are breaks in the temperature axis. The dashed vertical lines indicate T_c. The solid lines are least-squares fit to the expected theoretical behavior.

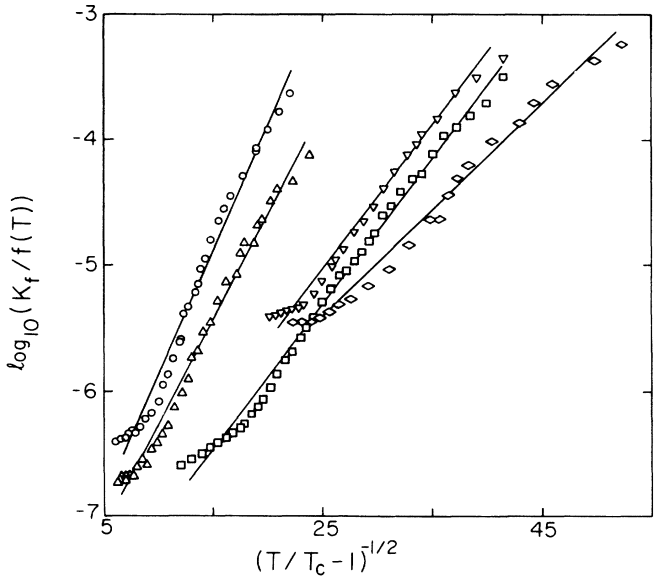

FIG. 12. Semilog plot of $K_f/f(T)$ in sec vs $t^{-1/2}$. Symbols correspond to film thickness as indicated in Fig. 6. The solid lines are least-squares fitted to the data analyzed via method two.

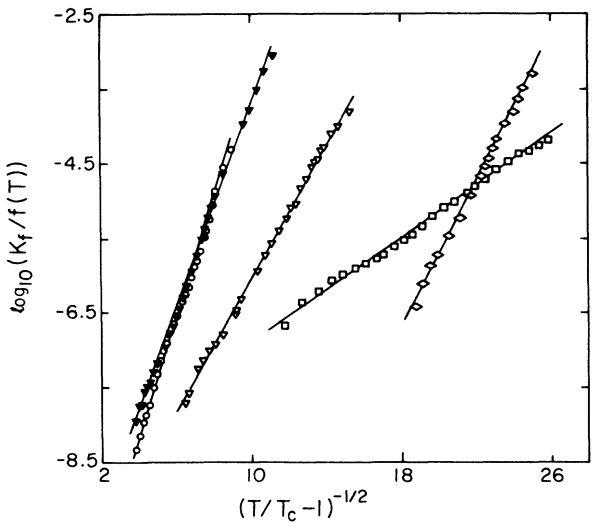

FIG. 13. Semilog plot of $K_f/f(T)$ in sec vs $t^{-1/2}$. Symbols correspond to film thickness as indicated in Figs. 5 and 6. The solid lines are least-squares fitted to the data analyzed via method one.

tionary plate can be monitored in a bridge network against a standard which is also located on the regulated plate of the cell. This gauge, which is calibrated when cold against a room-temperature gauge, has a typical reproducibility of 0.002 torr and a resolution about 10 times higher. The gauge contains sintered copper for thermal contact. It has an area of 5×10^4 cm^2, about 4% of the total area available to the helium.

D. Conductance of the empty cells

The thermal conductance of the empty cells was measured prior to condensing the helium sample. These data are shown in Fig. 4. The first cell, made mostly out of Mylar, shows a conductance in the range between 1 and 2×10^{-5} W/K. With the cross-sectional area of 0.15 cm^2 and distance of 1 cm, we obtained a conductivity of 1.0×10^{-4} W/cm K at 1.6 K. We are not aware of any measurements of thermal conductivity for Mylar at this temperature, but our result is comparable to a number of plastics. For the Kapton cell, in fact, at 1.6 K we also obtain a conductivity of 1.1×10^{-4} W/cm K. However, the conductance of this cell is much higher due to the larger cross-sectional area of the Kapton, 1.06 cm^2, and shorter distance between plates, 0.44 cm.

The conductance of the empty cell, plus, upon formation of a helium film, the contribution from the gas, should form the regular background conductance above which the singular, convective conductance of the film will be measured. We will discuss this in greater detail in the next section.

IV. DATA AND ANALYSIS

Data for our experiment have been taken over a period of several years. This involved the two experimental cells already described. Films were formed on Mylar, Kapton, and on an Argon-coated (25 Å) Mylar surface. The latter was done to investigate possible differences in film behavior when the substrate was coated with a noble gas. No difference was in fact found within the accuracy of our measurements. Films range in thickness between 11.7 and 156 Å above a non-superfluid layer. Prior to the present study, a series of measurements had also been reported for films on stainless steel.[35] These were more fruitful in studying the nonlinear aspect of the conductance[12] rather than the critical aspect of the transition discussed below. Measurements of mixture films[16] were also performed and will be discussed in a subsequent publication.

The measured conductance K_m for all the films for which we have a complete set of data are shown in Figs. 5 and 6. As discussed in the Introduction, K_m is bounded from above by a thermal resistance which is in series with the helium, and is bounded below by a resistance which is in parallel with the helium. Between these two bounds K_m varies over a range of three decades. Even before any analysis to extract the film conductance, it is clear that as one increases the film thickness the transition becomes sharper. Note that in Fig. 6 the temperature scale is expanded by a factor of 4. The implication of this sharpening is that if the data are described by Eq. (7), then the parameter b must increase with thickness.

To extract from these data the conductance due to the convective mechanism of the helium film, we examine the behavior of the upper and lower bounds. Values of the upper bound K_u as function of temperature are plotted in Fig. 7. The symbols with the error bars represent K_u for *different thickness films.* These correspond to data taken during the same cooldown. These data seem to be consistent with a T^3 dependence suggesting a Kapitza boundary resistance as the mechanism for K_u.[36] The

TABLE I. Results of the analysis with method two with T_c, b, and D/a^2 least-squares adjusted (see text). The standard errors for b are 2%, for D/a^2 they are 20%. The three thickest films are saturated and formed on a Kapton surface. The remaining films are for a Mylar surface. The 11.7 Å film is for a Mylar surface coated with 25 Å of argon. In the analysis, the data are corrected for film depletion, see text and Table II.

Thickness (Å)	T_c (K)	b	D/a^2 (10^9 sec^{-1})
11.7	1.2811	8.13	15
13.6	1.3683	8.0	6.0
14.7	1.3789	7.75	9.0
15.1	1.4593	9.73	6.2
16.5	1.5193	10.6	5.9
18.6	1.5720	13.4	1.5
19.1	1.5865	16.1	5.1
24.8	1.6200	16.9	0.73
26.8	1.8000	18.0	0.27
36.5	1.8759	34.0	1.1
50.6	2.0113	27.7	0.069
55.6	2.0292	32.8	0.082
95	2.1321	47.5	0.153
135	2.1504	49.9	0.059
156	2.1552	65.9	0.029

plusses in Fig. 7 represent data in a different cooldown taken with the *same thickness* film but extended over a broad temperature range below the transition. The dashed line through these data corresponds to a power-law dependence on T of 2.35 ± 0.05. This is also consistent with a boundary resistance rather than an impedance to gas flow. Our estimate of this flow impedance yields a value of K_u which is a factor of 100 larger than measured. Further, if K_u were due to gas impedance, it would have to vary more rapidly with temperature than we observed because the gas density depends on the pressure. In practice, because of the rapid variation in K_f near T_c, it is a good approximation over a narrow temperature range to use for K_u a constant value which can be determined at each individual film. In terms of the notation of Eq. (5), we have for $T<T_c K_f=\infty$, thus $K_K=K_u\sim$const.

To correct K_m for the lower bound is somewhat more problematical. The difficulty is shown in Fig. 8. Here we have plotted on a linear scale the measured conductance in the "tail" region above the transition. The solid line in this figure is the *calculated conductance* using the empty cell measurements, Fig. 3, and values of the *diffusive conductance* due to the helium gas.[37] The solid line misses the data by about 40%. Further, and more importantly, the temperature dependence is more rapid than expected, suggesting that it is associated with the film itself. These two problems become even more acute for thicker films with higher T_c's. This is not very obvious from Figs. 7 and 8 because of the logarithmic scale, but is very evident on a linear plot.

There are two ways in which we have analyzed the data near the lower bound. We assumed at first that the data determine its own lower bound and assumed that the critical behavior of K_f lies above this background. This is the dashed line in Fig. 8. K_f would then be the difference between the data and this line. Second, we assumed that we could *calculate* the lower bound as given by the solid line in Fig. 8. Consequently, the convective film conductance would now lie above this latter line. These two methods of analysis have a strong effect on the lower values of the film conductance, but do not affect the data close to T_c which have conductances 1000 times larger. We will report results using both methods of analysis. We note that one may view the first method as taking away from the data a temperature dependence which, in fact, is associated with the transition, but represents *higher order or less singular terms* than given by Eq. (7). The second method retains all the contribution to K_f, but makes it somewhat harder to isolate the most singular part. As we will see, these two possibilities affect our quantitative results for various parameters, but not the trends in these parameters which we want to emphasize. We note that T_c in particular is hardly affected by these analyses. In terms of the notation of Eq. (5), the two lines in Fig. 8 represent the quantity K_b. We remark that this difficulty in dealing with K_b is common to all measurements of film conductance. The choice of K_b represented by the dashed line in Fig. 8 has always been made. Our own alternative analysis with a calculated K_b can thus be used to assess how good this assumption is.

Results for K_f for some of our data as obtained via method one, the dashed line for K_b, are shown in Figs. 9 and 10. The data taken in one cooldown with the Mylar cell are shown here. We see now that the convective conductance K_f extends over about six decades near the transition. It is more apparent now that the critical region narrows as we move to thicker films and higher T_c's. For the film with T_c below 1.4 K, this region is nearly 100 mK wide. For the film with T_c near 1.8 K, this region is about 20 mK. For the thickest film for which we have measured K_f, 156 Å, this region is 3–4 mK.

The solid lines through the data in Figs. 9 and 10 represent a least-squares fit of the data to Eq. (7) with T_c, b, and D/a^2 as variational parameters. Further, as already discussed, the analysis corrects for film depletion in an iterative procedure (see the Appendix). Some results of this analysis have already been reported.[13] We note that the solid lines fit the data rather well over the full range of film thickness shown. Note that especially for

TABLE II. Results of the analysis with method one with T_c, b, and D/a^2 least-squares adjusted (see text). Standard errors are as indicated in Table I. Two entries are made for each parameter. The first is *before* a correction for film depletion, the second is *after* this correction is made (see text and the Appendix).

Thickness (Å)	T_c (K)		b		D/a^2 (10^9 sec^{-1})	
11.7	1.277	1.272	6.64	6.03	27	24
13.6	1.3660	1.3654	6.44	5.93	13	12
14.7	1.3708	1.3705	5.16	4.87	66	62
15.1	1.4579	1.4575	8.73	8.00	4.4	3.9
16.5	1.5184	1.5181	8.78	8.13	9.0	8.5
18.6	1.5699	1.5697	10.5	9.68	2.3	2.2
19.1	1.5860	1.5859	13.6	12.7	7.9	6.7
24.8	1.6188	1.6187	14.3	13.8	0.28	0.29
26.8	1.7981	1.7980	12.7	12.2	3.5	3.6
36.5	1.8751	1.8751	23.4	22.7	3.3	3.2
50.6	2.0117	2.0113	30.5	28.4	0.007	0.007
55.6	2.0292	0.0259	17.8	16.9	0.25	0.22

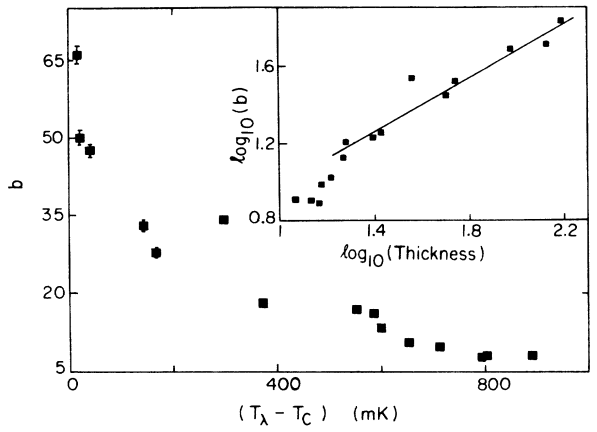

FIG. 14. The parameter b as a function of $T_\lambda - T_c$. Inset: log-log plot of b vs film thickness. The solid line is a least-squares fit to the data for thickest films.

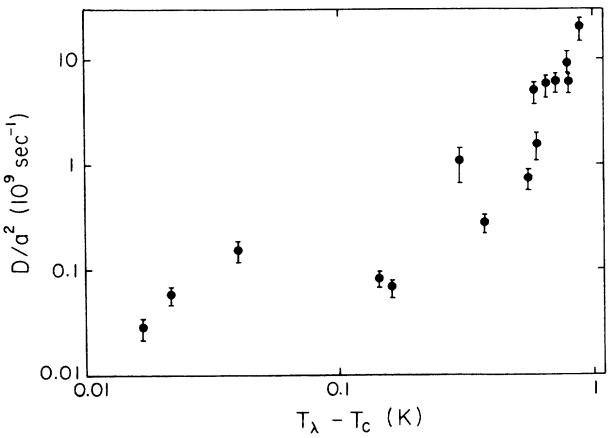

FIG. 16. The parameter D/a^2 in sec^{-1} vs $T_\lambda - T_c$ on a log-log plot.

the thin films T_c's, the dashed vertical lines in these figures, are substantially below the last data point. Thus, even at conductances of the order of 1 W/K ($\sim 10^4$ W/K cm for a 13.6 Å film), one is still not very close to T_c. Measurements in this region are extremely difficult because the conductivity becomes more strongly power dependent and measurements in the limit of $Q=0$ involve very small values of ΔT.

A more telling way of showing how well the data fit the expected theoretical relation, Eq. (7), is to plot these data versus $t^{1/2}$. Such a plot of these data is shown in Fig. 2 of Ref. 13. Again, one finds excellent fits to Eq. (7) with deviations only for a few points close to T_c or far from T_c. These deviations are expected (and visible as well in Figs. 9 and 10), close to T_c because of the difficulty in measuring K_m, and far from T_c, because of the sensitivity to the choice of background, or because of being too far from the asymptotic region in which Eq. (7) is expected to hold.

We discuss next the analysis according to method two, i.e., using the calculated value for K_b. We write Eq. (7) for the film conductance in the form

$$K_f = \left[\frac{a^2}{D}\right] f(T) \exp\left[\frac{4\pi}{b} t^{1/2}\right], \tag{11}$$

where $f(T)$ is a weak temperature-dependent function involving the latent heat. This can be calculated using our measurements of pressure. An extra factor of film thickness d would appear in Eq. (10) if one were to calculate the conductivity rather than conductance. The function $f(T)$ contains the geometrical factors of the perimeter over which the film flows and the distance between top and bottom plates of the cell. The constant F, which ap-

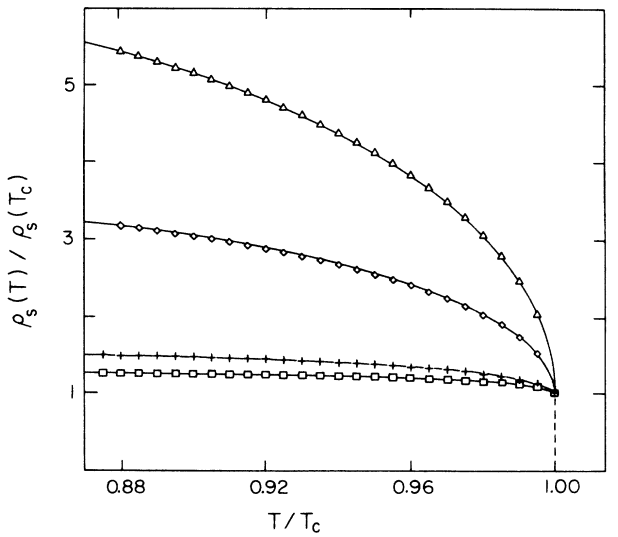

FIG. 15. The ratio $\rho_s(T)/\rho_s(T_c)$ as a function of T/T_c, for various values of the parameter b. From the lowest to the highest these correspond to films with $b=5$, 8, 30, 60, or T_c approximately of 1, 1.3, 2 and 2.1 K.

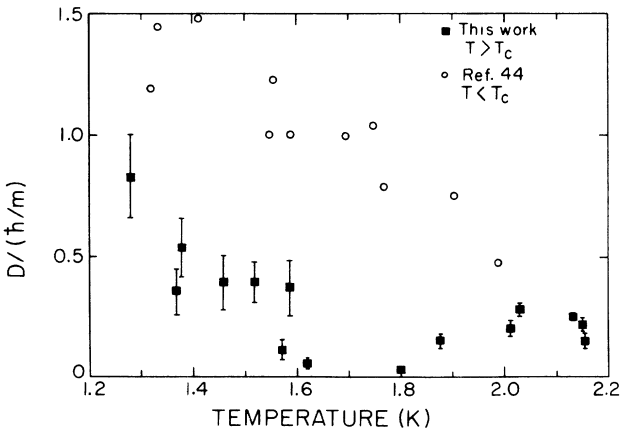

FIG. 17. The diffusion constant D in units of $\hbar/m$ vs temperature. The open circles for $T < T_c$ are from Ref. 44. To obtain D from our data we have assumed that the core parameter is equal to the three-dimensional correlation length. See text.

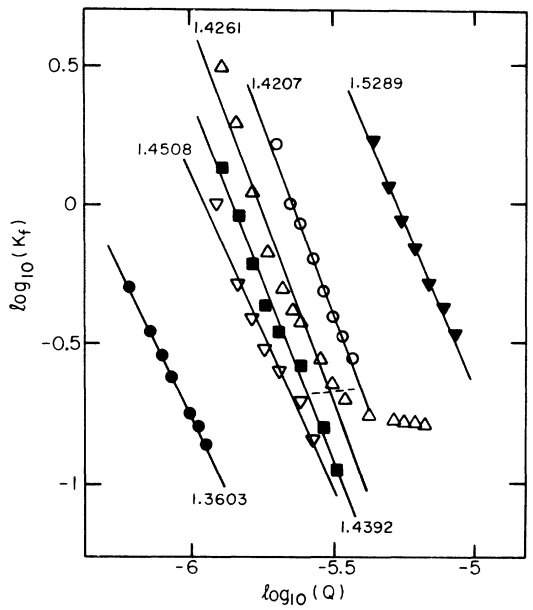

FIG. 18. Power dependence studies for $T < T_c$. K_f is in W/K and Q in W. The symbols refer to ▽, △, ●, ■, $h = 14.1$ Å; ▼, $h = 18.6$ Å, ○, $h = 13.6$ Å.

pears in Eq. (7), has been assumed to be one. We see now that the quantity $K_f/f(T)$ can be least-squares fitted to extract D/a^2, b, and T_c. This was done to obtain the solid lines in Figs. 9 and 10. The results of doing this for method two, using the *calculated value* for K_b, are shown in Figs. 11 and 12. These are semilog plots of $K_f/f(T)$ vs $t^{-1/2}$. On these plots the data are expected to fall on straight lines. We can see that this behavior is followed

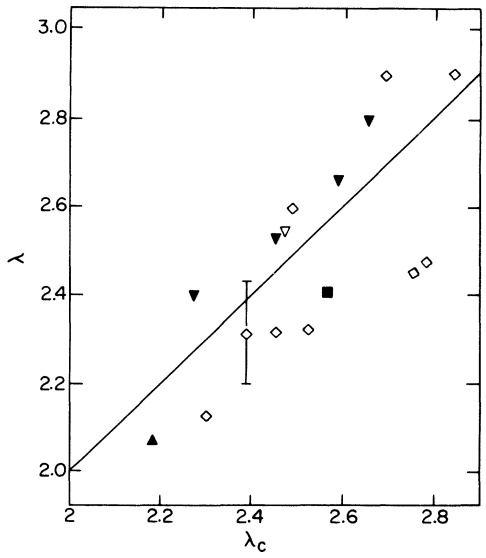

FIG. 19. The value of the exponent of the power dependence of the conductance λ vs the *expected* exponent λ_c on the basis of the behavior of K_f above T_c. These exponents scatter about a 45° line. The error bars for one point are representative of all the other. Symbols refer to film thickness as indicated in Fig. 5.

by the data in a reasonable way; but there are clearly systematic deviations for low values of K_f. These can be traced to our calculated values of K_b as done for this method of analysis. We show for comparison in Fig. 13 five sets of data spanning the full range of film thicknesses and for which K_b is chosen as in method one. These fits now show no systematic residuals. In spite of this, we feel that method two is more logically consistent in the sense that there is no mechanism associated with the gas which would give the relatively rapid temperature dependence measured. Thus, it seems more reasonable to attribute it to the film. It is possible that a more complete temperature dependence for the two-dimensional correlation length would contain higher-order terms to take care of these systematic residuals. We find that the fitting parameters which are obtained in method two are better behaved and scatter somewhat less than for method one. We have summarized the numerical results from both of these analyses in Tables I and II. In the second table we also show results for the unsaturated films before and after corrections for vaporization. One can see from this table that the trends in fitting parameters are not affected by this analysis. The magnitude of T_c in particular is hardly changed. We now discuss the parameter b, D/a^2, and T_c.

A. The parameter b

This parameter appears as a nonuniversal constant in the KT theory for the divergence of the correlation length for $T > T_c$ [see Eq. (6)]. This parameter also describes the magnitude of the $t^{1/2}$ cusp in the superfluid density as one approaches T_c from below. A value for b can be obtained in terms of the ratio E_c/T_c, where E_c is the vortex core energy.[38] Such a relationship, however, fails for thicker films because of the assumption that the superfluid density be nearly temperature independent near T_c. A more general relationship was recently obtained which incorporates a T_c (hence thickness) dependence in b via the background (nonvortex) superfluid density.[39] All of these relationships do not calculate b but rather give b in terms of other nonuniversal quantities.

In the first publication of our work we suggested that the increase of b may, in fact, be related to the three-dimensional correlation length, ξ_{3D}.[13] Petschek has suggested a way in which b should scale with size.[40] He argues that E_c should scale with ξ_{3D} and that the difference between normal and superfluid free energy should scale as ξ_{3D}^{-3}. This, plus finite-size scaling[41] of T_c, $(T_\lambda - T_c) \sim d^{-1/\nu}$, yields

$$b \sim d^{1/2\nu} . \tag{12}$$

Our results for the parameter b are shown in Fig. 14. We have plotted these on a linear scale versus $T_\lambda - T_c$ where T_λ is the bulk, 3D transition. The increase in b as $T_c \to T_\lambda$ (or as d increases) is obvious from this plot. This is a reflection of the slope of the lines in Figs. 11 and 12 becoming smaller. From Fig. 14 we see that the scatter in the value of b is larger than the statistical error which is of the order of the size of the symbols. This is typical for these data whether analyzed with method one or two.

In the inset of Fig. 15, we have a log-log plot of b vs d.[42] We have fit a straight line through the data of thicker films in the region where the scaling arguments might apply. We find an exponent of 0.69 ± 0.01. This is to be compared with $1/2\nu=0.74$. We view this as qualitative agreement. We do not feel, in particular, that Eq. (11) provides a strong test of finite-size scaling. First of all, the arguments leading to 11 are not as straightforward as, for instance, the shift in T_c with d. Second, even though the statistical error in b is only 2%, the accuracy with which b can be obtained experimentally is not very high. This can be seen from the scatter of b in Fig. 14. The values of b as obtained with both methods of analysis are given in Tables I and II.

The implications of the increase of b as far as the 2D superfluid density near the transition can be obtained from[18]

$$\frac{\rho_s(T)}{T}=\frac{\rho_s(T_c)}{T_c}\left[1+\frac{b}{4}t^{1/2}\right]. \tag{13}$$

We have calculated the superfluid density for b's in the range of 5–60 corresponding to T_c's between 1 and 2.1 K. This is plotted in Fig. 15. We can see that at higher T_c's there is a strong temperature dependence of ρ_s near the transition. This, in addition to the strongest temperature dependence of the background $\rho_{s0}(T)$, which is *not included* in this figure, would make it very difficult to extract the universal jump in ρ_s at T_c for thick films.

B. The parameter D/a^2

The ratio of the diffusion constant to the square of the vortex core radius is obtained from the prefactor of Eq. (10). In terms of the plots in Figs. 13 and 14, D/a^2 is related to the $t^{-1/2}=0$ intercept of the fitted straight line. The absolute value with which D/a^2 can be obtained is related to the accuracy with which we know $f(T)/d$. We believe this is about 10%. More importantly, however, in Eq. (10) the unknown proportionality constant between free vortex density and correlation length, see Eq. (7), has been set equal to one. Thus, we would say that the absolute value of D/a^2 can be obtained from our analysis within a factor of order unity.

Our results for this parameter are plotted versus $T_\lambda-T_c$ on a log-log scale in Fig. 16. The general trend in D/a^2 is a decrease by about three decades as one proceeds from the thinnest films to the thickest. This decrease might be expected both from the behavior of D and a. The diffusion constant is a measure of the ability of vortices to move along the film.[18] This is influenced by interactions with the substrate, which may give a nonuniversal character to D, and interactions with thermal excitations. These latter increase with temperature which would tend to decrease D. Further, D is inversely proportional to the square of the background superfluid density which also increases as the film thickness increases. For all these reasons, one would expect D to decrease as the films become thicker, i.e., as T_c approaches T_λ.

The vortex core parameter is expected to be proportional to the 3D correlation length. This quantity increases as $T_c\rightarrow T_\lambda$, eventually diverging with a characteristic exponent $\nu=0.672$. This would also make D/a^2 decrease. To obtain D, we have assumed that $a=\xi_{3D}$, and we have calculated the 3D correlation length from the superfluid density.[43] This value of D is plotted in units of $\hbar/m$ versus temperature in Fig. 17.

Our data suggest that D does indeed decrease as the films' transition temperature approaches T_λ. However, there is clearly not enough accuracy in these results to establish a functional form for D. One may even conclude that $D\sim\text{const}=0.3\hbar/m$. Plotted in this figure are also results for D obtained by Adams and Glaberson.[44] These are direct measurements of D for T approaching T_c *from below*. Our results are for T approaching T_c *from above*. Both of these results show similar trends. A comparison of the absolute magnitude is not warranted since our results are only within a factor of order unity.

We note as well that in Ref. 44, as well as 45, it is found that D has a power-law temperature dependence as $T\rightarrow T_c^-$. In our analysis for $T\rightarrow T_c^+$, we assumed that $D=$const. In fact, because of these results and the calculation of Huber,[46] we incorporated a power-law temperature dependence in D as suggested in Ref. 46. We find that the parameters b and T_c are charged insignificantly. For D/a^2, the change is more substantial but still within the error bars shown in Fig. 17. The reason for such small effect is that any power-law dependence introduced in the prefactor of the exponential behavior of K_f is not of much consequence.

C. The critical temperature, T_c

The critical temperature is the parameter determined most precisely from our data. It is relatively insensitive to how the data are reduced or the method of analysis. See Tables I and II. The change in the quantity $T_\lambda-T_c$ as a function of the film thickness should be governed, according to finite-size scaling, by the exponent of the 3D correlation length. A report on this aspect of our work has been published already.[4] Here we only remark that *this scaling does not work* and that this conclusion is independent of how we analyze the data.

D. Power studies for $T<T_c$

As discussed in the Introduction, below T_c one expects a dependence of K_f on the velocity of film flow. This implies for a depairing mechanism that $K_f\sim Q^{-\lambda}$, where $\lambda=\frac{1}{2}(4+bt^{1/2})$. We have checked this dependence for a number of films in the velocity range $\sim10^{-2}$–10^{-3} cm/sec, for which the restriction $r_c\gg\xi_-$ is well satisfied. Some of these data are shown in Fig. 18.[47] Here the film conductance is plotted versus the power applied on a log-log scale. Data for three different films are shown at temperatures below T_c. The corresponding film velocities depend inversely on the film thickness. Given the geometry of our cell, a power of 10^{-6} W corresponds to 2×10^{-3} cm/sec for a 16 Å film.

The data in Fig. 18 were least-squares fitted resulting in the straight lines shown through the data. These fits are

reasonable although the range of data, ~ 1 decade in K_f, is not very large. These data, as well as other, indicate that the expected power law is observed irrespective of the thickness or the separation from T_c. Also, for a given coverage, as the transition is approached, a smaller amount of power is needed to generate the same free vortex density. This is consistent with a picture where the energy required to unbind vortex pairs becomes progressively smaller as T_c is approached. We have, in addition, data which extend to higher powers and lower values of K_f. Some of these data are shown below the dashed line as the up triangles. These data deviate sharply from a power-law dependence. It appears that at higher values of Q, a finite velocity field is not as effective in lowering K_f as for small velocities. A type of saturation seems to be taking place, even though we are still well within the criterion of $r_c \gg \xi_-$.

The value of the slopes in the power-law plots is the quantity we have called λ. This quantity can also be *calculated* using the value of b and T_c determined from the exponential dependence of K_f *above* T_c. We call this calculated value λ_c. We plot in Fig. 19 λ vs λ_c. If the theory were correct and the data very precise, the data should fall on a line of slope one going through the origin. This is the line which is drawn in Fig. 19. We see that the data scatter about this line within a band of about $\pm 10\%$. We consider this quite reasonable given the precision with which b can be determined. Note that the data in Fig. 19 represent different films thickness and different temperatures. We believe this represents the first check of this kind for the parameter b obtained independently from the conductance for $T > T_c$ and the Q dependence obtained for $T < T_c$. We remark that the results shown in Fig. 19 are for what we have called method one of data analysis for $T > T_c$. Had we used method two, the data would tend to lie somewhat below the line and the agreement would not be as good.

The data were also tested for a depinning mechanism.[21,22] One finds good agreement with this mechanism as well over a considerable range of powers. However, the size of the pinning site as extracted from the fits seems rather large. Pinning sites of the order of 10^4 Å are required.[25]

V. COMPARISON WITH OTHER EXPERIMENTS

There have been many experiments in which the thermal conductivity of ^{4}He films near the transition has been measured.[9–12] These have been done with films formed on a variety of substrates, with different experimental arrangements and emphasis on different features of the transition. Broadly speaking, there have been two principal areas of investigation: the nonlinear dependence of the film conductance on power for $T < T_c$, and the linear dependence for $T > T_c$. This latter, which tests the divergence of the 2D correlation length, has been the principal focus of this paper. We compare this with other results.

The earliest measurements to show an exponential divergence of K_f were those of Liebenberg[48] and Ratman and Mochel.[49] The first were for a saturated film, the latter were for a film with $T_c \simeq 1.25$. These latter data were originally analyzed with an activation-type expression and, subsequently, by Teitel according to Eq. (4).[23] He finds that the data obey this equation with $b \leq 4$ over a region of about a decade of K_f. This value of b, as can be seen from Fig. 14, is in reasonable agreement with our own results.

Agnolet *et al.* have reported measurements of a single film with $T_c \simeq 1.28$ K.[10] This film was formed on Mylar and a four-terminal technique was used to measure the conductance. This was obtained over a range of seven decades. Their data yield $b = 6.96$, while $D/a^2 = 6.39 \times 10^{11}$ sec^{-1} if, in keeping with our own assumptions, one takes F to be unity. A correction of these data for evaporation effects gives $b = 4.65$ and D/a^2 remains unchanged. The value of b is in good agreement with our own results. D/a^2, however, is larger than expected when compared with the results in Fig. 16. In fact, their value of D/a^2 is in better agreement with our own when compared with results of using the first method of analysis. This is a more meaningful comparison since this is the kind of analysis used in Ref. 10.

Maps and Hallock[9] measured film conductance in a different arrangement from our own or that of Ref. 10. The film was formed on a Mylar strip suspended in an open chamber with isothermal walls. This is a similar geometry as for Refs. 11 and 24. The film conductance for seven films with T_c's in the region between 1.3 and 1.6 K was obtained. This was done by varying the thickness at a fixed temperature. These data yield a constant value of $b \simeq 3 \pm 0.5$. This is somewhat low when compared to our results, and does not show the T_c dependence in Fig. 13. We would expect that b would change by about a factor of 2 in this range of T_c. The value we obtain at $T_c \simeq 1.6$ is about 16. For D/a^2 these data yield values in the range 10^{12}–10^{11} sec^{-1}. This is in close agreement with the single measurement of Agnolet *et al.*,[10] but is more than two decades higher than values in Fig. 15, and is also higher than values obtained with our method one. There is, however, a slight trend toward smaller values of D/a^2 with higher T_c's which is consistent with our own observations.

Joseph and Gasparini studied the conductance for films formed on a stainless steel substrate.[12] Of the two cells for which they obtained data, cell 3 is the one of comparable design to the ones discussed in the present work. They obtain for b values which increase from 7.6 to 11 in the range of 1.63–1.75 K. For D/a^2 they find in the same range a decrease from 2×10^9 to 4×10^7 sec^{-1}. These trends are in the right direction when compared to the present work, but are somewhat lower than values in Figs. 14 and 16. We remark that their data can be analyzed only over a limited range in K_f, 2–3 decades, and that the stainless steel surface is likely to give different values for their parameters, at least D/a^2, when compared to Mylar. The stainless steel substrate is not as smooth as Mylar. Indeed, their work for the nonlinear dependence of the conductance on power shows that a depinning mechanism seems to be dominant as opposed to a depairing mechanism as seen for films on Mylar in this work, as well as in Refs. 9 and 24.

Hess and Muirhead[11] measured the superfluid behavior of films on various substrates. In particular, for a gold-plated copper substrate they obtain the film conductance for the linear region. Their data are obtained for a thermodynamic path similar to Ref. 9. The temperature is fixed and the film thickness is varied. From the analysis of the films, they obtain $D/a^2 \sim 10^8 - 10^9$ sec^{-1} and $b = 14 - 12$. This for T_c's in the range of 1.155–1.485 K. The trend in these parameters is contrary to our own observations, but it is not clear that this is significant, since the range of data over which the exponential divergence is tested is very limited, one to two decades.

VI. SUMMARY AND CONCLUSIONS

We have reported measurements and analysis of the convective conductance of ^{4}He films near the superfluid transition. These data span a region of temperatures from 1.28 to 2.16 K and film thickness from 11.7 to 156 Å. The main goals of our work are, first of all, the verification of the dynamic theory predictions for the convective conductance at the Kosterlitz-Thouless transition and, second, to see how parameters in this theory are renormalized as T_c approaches T_λ.

We find that there are two consistent ways of analyzing our data. These are associated with how one treats the lower bound of the measured conductance. Both methods yield reasonable fits to the expected theoretical expressions, one method being slightly better than the other. These two methods affect the resulting parameters, especially D/a^2, but do not affect the trends which we wish to emphasize. These trends are that b increases with T_c while D/a^2 decreases. The behavior of b is consistent with a growth which parallels the 3D correlation length. Empirically, the growth of b is a reflection of the fact that the film is 2D in character over a progressively narrower temperature region as the film thickness increases. We find that the parameter b, obtained from $T > T_c$ by fitting the data to the exponential divergence, is consistent with the parameter b as obtained from the nonlinear dependence of the conductance on power for $T < T_c$. We have shown in Fig. 15 the implications which a large value of b has on the behavior of the superfluid density.

For the parameter D/a^2, the decrease with thicker films makes physical sense both on the basis of the behavior of D and of a^2. If we take a^2 as the square of the 3D correlation length, we can calculate D for $T > T_c$ and compare with direct measurements of the diffusion constant for $T < T_c$. We find that both of these data show a D which decreases as T_c approaches T_λ. In our own case, however, the scatter is such that a constant value of D would also be a reasonable interpretation. The absolute value of D cannot be compared since, from our analysis, we can only determine D to within an unknown factor of order unity.

Our analysis of the shift in transition temperature T_c as a function of film thickness, and the implications vis-a-vis finite-size scaling were discussed in an earlier publication. We remark here that *the conductance we measured for our thickest film shows no evidence of dimensionality crossover.* Even for the thickest films we have studied, with T_c 15 mK from T_λ, the smallest value of conductance that we measure is several decades above the highest measured diffusive conductance for bulk helium above T_λ. Thus, we see no evidence of a crossover in temperature dependence from a power law to an exponential.

We have compared our work with earlier results. We find good qualitative agreement but not at the level that one would wish. The lack of complete agreement is to a great extent due to the difficulty in measuring the very singular behavior of K_f over a wide range of T-T_c to extract the critical behavior. It seems clear to us that a new generation of experiments should be planned utilizing thermometers of higher resolution and cells which allow a wider range of conductance to be accessible. This would resolve the ambiguities in the method of analysis, allow for a more detailed study of the power dependence, and possibly obtain behavior showing 3D to 2D crossover.

ACKNOWLEDGMENTS

We would like to thank Mr. R. J. Theis of E. I. Dupont De Nemours and Company for providing us with the Mylar, and Dr. D. S. Greywall of AT&T Bell Laboratories for giving us the silver diaphragm for our pressure gauge. One of us (D.F.) acknowledges support from Universidad Nacional Autonoma de Mexico. This work was supported by the National Science Foundation, Low Temperature Physics Program under Grant Nos. DMR8305742 and DRM8601848.

APPENDIX

1. Differential temperature measurement

We consider the situation of Fig. 1 where we apply a heat input to the bottom plate of the experimental cell and want to measure the resulting temperature difference. We define $r_1(T)$, $r_2(T)$, and $R(T)$ as the resistances of the top and bottom thermometers and the bridge ratiotransformer setting at equilibrium. These are related as

$$r_1(T) = R_0(T) r_2(T) , \tag{A1}$$

where we denote by $R_0(T)$ the setting corresponding to zero-power input on the bottom plate, $Q = 0$. Let us now consider $Q \neq 0$, and assume that both top and bottom thermometer suffer a shift in temperature $\delta T_1, \delta T_2$. In principle, the regulated top thermometer should remain constant, but we assume for generality that $\delta T_1 \neq 0$. Using

$$r_1(T + \delta T_1) = R r_2(T + \delta T_2) , \tag{A2}$$

and

$$\frac{dr_1}{dT} = R_0 \frac{dr_2}{dT} + r_2 \frac{dR_0}{dT} , \tag{A3}$$

we obtain upon Taylor-series expansion of (A2)

$$\delta T_2 = \left[R\frac{dr_2}{dT} \right]^{-1} \left[(R_0 - R) r_2(T) + \delta T_1 \left[r_2(T)\frac{dR_0}{dT} + R_0 \frac{dr_2}{dT} \right] \right] . \tag{A4}$$

Thus, the temperature difference, $\Delta T = \delta T_2 - \delta T_1$, between top and bottom plates is given by

$$\Delta T = \left[\frac{R_0}{R} - 1 \right] \left[\frac{1}{r_2}\frac{dr_2}{dT} \right]^{-1} + \delta T_1 \left[\frac{1}{R}\frac{dr_2}{dT} \left[\frac{1}{r_2}\frac{dr_2}{dT} \right]^{-1} + \frac{R_0}{R} - 1 \right] . \tag{A5}$$

The first term in the above is the leading-order term. The second, which involves δT_1, represents a correction in case the regulation slips, or if some of the heat applied to the bottom plate travels through the leads of the top thermometer to the cold sink at the ^{4}He evaporator. We find empirically that the second term gives $\lesssim 1\%$ correction at large powers. When necessary, as when doing power studies, we correct for this. In practice, the important data for film conduction is in the limit of $Q = 0$, hence the leading term in (A5) is sufficient

2. Film depletion

As the temperature increases, the pressure of the gas in equilibrium with the film also increases. Then, in a closed system where the amount of helium is fixed, as the temperature is raised, an unsaturated film will thin. The rate at which such thinning takes place depends largely upon the surface to volume ratio of the experimental cell. To display more explicitly the thickness dependence, we write the conductivity as follows:

$$K_f = f(T) d^{-1} \exp[at(d)^{-1/2}] , \tag{A6}$$

where $f(T)$ is a function that depends on temperature through the latent heat, and d is the film thickness. The total differential along a thermodynamic path where both T and d change is

$$dK_f = (\partial K_f/\partial T)_d dT + (\partial K_f/\partial d)_T dd . \tag{A7}$$

For small ΔT, Δd we write

$$\Delta K_f = (\partial K_f/\partial d)_T \Delta d + (\partial K_f/\partial T)_d \Delta T . \tag{A8}$$

The first term on the right-hand side of (A8) represents the correction to the film conductance due to the change in the film thickness. We derive below an expression for this term.

Taking the derivative of (A6), we have

$$K_f^{-1}(\partial K_f/\partial d)_T = -d^{-1} + (aT/2T_c^2)(T/T_c - 1)^{-3/2} \times (dT_c/dd) , \tag{A9}$$

where dT_c/dd may be obtained from experimental data and, in terms of the notation in the Introduction, $a = 4\pi/b$. We have ignored in (A9) the weak dependence of $f(T)$ on thickness. In the analysis of the data, however, we take this into account by calculating $f(T)$ for every point. We now expand $d(T)$ near T_c,

$$\Delta d(T) = d(T_c) - d(T - T_c) \simeq -(T - T_c)\frac{dd}{dT} . \tag{A10}$$

We can relate the thickness to the number of moles of helium by treating the gas as ideal (a more precise expression using the second virial coefficient has no effect on the analysis),

$$\frac{dd}{dT} = \left[\frac{V}{RT} \right] \left[\frac{dP}{dT} - \frac{P}{T} \right] \frac{dd}{dn} , \tag{A11}$$

where V is the volume available to the gas. The correction term can now be written as

$$\left[\frac{\partial K_f}{\partial d} \right]_T \simeq -\left[\frac{VK_f}{RT} \right] \left[-d^{-1} + \left[\frac{aT}{2T_c^2} \right] \left[\frac{T}{T_c} - 1 \right]^{-3/2} \left[\frac{dT_c}{dd} \right] \right] \left[\left[\frac{dP}{dT} \right] - \frac{P}{T} \right] (T - T_c) \left[\frac{dd}{dn} \right] . \tag{A12}$$

Now what is measured is the dependence of the conductivity on temperature modified slightly due to a change in film thickness. Since we are interested only in the temperature dependence, the thickness dependence as indicated (to a first approximation) in (A12) should be removed. We can write this as

$$K_{\rm corr} \simeq K_f \left\{ 1 + \left[\frac{V}{RT} \right] \left[\frac{dd}{dn} \right] \left[-d^{-1} + \left[\frac{aT}{2T_c^2} \right] \left[\frac{T}{T_c} - 1 \right]^{-3/2} \left[\frac{dT_c}{dd} \right] \right] \left[\left[\frac{dP}{dT} \right] - \left[\frac{P}{T} \right] \right] (T - T_c) \right\} , \tag{A13}$$

where K_f is measured film conductance. In (A13), (dd/dn) is a function of the surface area and is determined from the amount of helium needed to form, say, one layer or 3.6 Å of film. Since the second term in (A13) is positive, $K_{\rm corr} > K_f$. This is understandable since, if the film thins, its T_c will shift towards lower temperatures. As the measurements are performed farther away from T_c, the measured conductance will be smaller than what would be measured for a constant film thickness. This implies that K_f, when the film is allowed to thin, is

sharper than the true conductance. We note that the correction is singular at T_c. That is, in spite of the fact that thickness changes are very small near T_c, the correction is larger because of the singular dependence of K_f. Finally, we note that the correction involves T_c and a, which are not known *a priori*. Thus, the correction involves an iterative procedure.

The data were analyzed in the following way. The film conductance was extracted from the measurements and it was divided by the latent heat and geometrical ratio as discussed in data analysis. A three-parameter least-squares fit to the data was performed. From the fit, the parameters T_c and $a = 4\pi/b$ were extracted and substituted in (A13) to calculate the corrected conductance. This was again least-squares fitted, and new parameters T_c and $a = 4\pi/b$ extracted. The iterative procedure is repeated until T_c and b do not change. In all cases, this takes at most three iterations.

We note that this thinning correction leaves the data as K_f along a path of constant thickness but with a slightly different thickness at different values of T-T_c. A further correction is needed involving changes of K_f at constant T-T_c due to the fact that parameters b and D/a^2 change with d. We expect, however, this correction to be small since these parameters vary little within the range in which d changes. Details of how the thinning correction affects the results can be found in Table II.

Finally, we note that the correction we have outlined is completely analogous to what is done in extracting the heat capacity at constant chemical potential from the heat capacity at constant concentration in ^{3}He–^{4}He mixtures. The details of the functional forms are, of course, different.

---

*Present address: Department of Physics, Kent State University, Kent, OH 44242.

†Present address: Department of Physics, Syracuse University, Syracuse, NY 13244.

[1]W. M. Fairbank, M. J. Buckingham, and C. F. Kellers, in *Proceedings of the Fifth International Conference on Low Temperature Physics and Chemistry,* edited by J. R. Dillinger (University of Wisconsin Press, Madison, Wisconsin, 1958). For the most recent measurements, see J. A. Lipa and T. C. P. Chui, Phys. Rev. Lett. **51**, 2291 (1983). For a review, see G. Ahlers, in *The Physics of Liquid and Solid Helium,* edited by K. H. Bennemann and J. B. Ketterson (Wiley, New York, 1976), Pt. I.

[2]J. M. Kosterlitz and D. J. Thouless, J. Phys. C **6**, 1181 (1973); J. M. Kosterlitz, *ibid.* **7**, 1046 (1974).

[3]A. N. Berker and D. R. Nelson, Phys. Rev. B **19**, 2488 (1979).

[4]Y. Y. Yu, D. Finotello, and F. M. Gasparini, Phys. Rev. B **39**, 6519 (1989).

[5]J. R. Clow and J. D. Reppy, Phys. Rev. Lett. **16**, 887 (1966); J. A. Tyson and D. H. Douglass, Jr., *ibid.* **17**, 472 (1966); D. S. Greywall and G. Ahlers, Phys. Rev. A **7**, 2145 (1973). For a review, see G. Ahlers, *ibid.* **7**, 2145 (1973).

[6]I. Rudnick, Phys. Rev. Lett. **40**, 1454 (1978).

[7]D. J. Bishop and J. D. Reppy, Phys. Rev. Lett. **40**, 1727 (1978).

[8]G. Ahlers, Phys. Rev. Lett. **21**, 1159 (1968); W. Y. Tam and G. Ahlers, Phys. Rev. B **32**, 5932 (1985); J. A. Lipa and T. C. P. Chui, Phys. Rev. Lett. **58**, 1340 (1987).

[9]J. Maps and R. B. Hallock, Phys. Rev. Lett. **47**, 1533 (1981); Phys. Rev. B **26**, 3979 (1982).

[10]G. Agnolet, S. L. Teitel, and J. D. Reppy, Phys. Rev. Lett. **47**, 1537 (1981).

[11]G. B. Hess and R. J. Muirhead, J. Low Temp. Phys. **49**, 481 (1982).

[12]R. A. Joseph and F. M. Gasparini, Physica (Amsterdam) B&C **109&110**, 2102 (1982).

[13]D. Finotello and F. M. Gasparini, Phys. Rev. Lett. **55**, 2156 (1985).

[14]V. Dohm, J. Low Temp. Phys. **69**, 51 (1987).

[15]For a recent review on finite-size scaling, see M. N. Barber, in *Phase Transitions and Critical Phenomena,* edited by C. Domb and J. L. Lebowitz (Academic, New York, 1983), Vol. 8.

[16]D. Finotello, Y. Y. Yu, and F. M. Gasparini, Phys. Rev. Lett. **57**, 843 (1986).

[17]D. R. Nelson and J. M. Kosterlitz, Phys. Rev. Lett. **39**, 1201 (1977).

[18]V. Ambegaokar, B. I. Haperin, D. R. Nelson, and E. D. Siggia, Phys. Rev. Lett. **40**, 783 (1978); Phys. Rev. B **21**, 1806 (1980).

[19]B. A. Huberman, R. J. Myerson, and S. Doniach, Phys. Rev. Lett. **40**, 780 (1978).

[20]J. L. McCauley, Phys. Rev. Lett. **45**, 467 (1980).

[21]D. A. Browne and S. Doniach, Phys. Rev. B **25**, 136 (1982).

[22]L. Yu, Phys. Rev. B **25**, 198 (1982).

[23]S. L. Teitel, J. Low Temp. Phys. **46**, 77 (1982); Ph.D. thesis, Cornell University, 1981.

[24]S. G. Hedge, R. A. Cordery, and W. I. Glaberson, Phys. Rev. B **26**, 2690 (1982).

[25]D. Finotello, Ph.D. thesis, State University of New York at Buffalo, 1985.

[26]Both Mylar and Kapton are registered trademarks of the E. I. DuPont De Nemours and Co.

[27]Emerson Cumming, Inc., Canton, Massachusetts.

[28]V. Steinberg and G. Ahlers, J. Low Temp. **53**, 255 (1983).

[29]Nuclepore Corporation, Pleasanton, California 94586.

[30]T. P. Chen, M. J. DiPirro, A. A. Gaeta, and F. M. Gasparini, J. Low Temp. Phys. **26**, 927 (1977).

[31]Y. Y. Yu, Ph.D. thesis, State University of New York at Buffalo, 1988.

[32]F. G. Brickwedde, H. van Dijk, M. Durieux, J. R. Clement, and J. R. Logan, *The 1958 ^{4}He Scale of Temperatures* (U.S. Government Printing Office, Washington, D.C., 1960).

[33]E. Zair and A. J. Greenfield, Rev. Sci. Instrum. **44**, 695 (1973).

[34]D. S. Greywall and P. A. Busch, Rev. Sci. Instrum. **51**, 509 (1980).

[35]R. Joseph, Ph.D. thesis, State University of New York at Buffalo, 1982.

[36]For a discussion of the Kapitza resistance, see, for instance, J. Wilks, *The Properties of Liquid and Solid Helium* (Oxford University Press, Oxford, England, 1967).

[37]K. Fokkens, N. Vermeer, K. W. Taconis, and R. De Bruyn Ouboter, Physica **30**, 2153 (1964).

[38]A. J. Dahm, Phys. Rev. B **29**, 484 (1984).

[39]G. Agnolet, D. McQueeney, and J. Reppy, Phys. Rev. B **39**,

8934 (1989).

[40]R. G. Petschek, Phys. Rev. Lett. **57**, 501 (1986).

[41]M. E. Fisher, in *Critical Phenomena,* Proceedings of the International School of Physics "Enrico Fermi," Course LI, Verenna, 1970, edited by M. S. Green (Academic, New York, 1971). For a recent review of finite-size scaling, see M. N. Barber in *Phase Transitions and Critical Phenomena,* edited by C. Domb and J. L. Lebowitz (Academic, New York, 1983), Vol.8.

[42]Our film thickness is determined as follows. From the total helium condensed, we subtract the number of moles in the gas and the nonsuperfluid layer. The residual is assumed to form a superfluid film on all surfaces. The surface is mostly due to the Nuclepore filters. The thickness on Mylar surface of the cell is given by $d=d_N(\alpha_M/\alpha_N)^{1/3}$, where d_N is the thickness on Nuclepore and the α's are the van der Waals constants, $\alpha_M=2.7\times10^{-37}$ erg cm^3, $\alpha_N=2.4\times10^{-37}$ erg. For details on how the thickness of the saturated films are calculated, see Ref. 4. Note that the thickness of the unsaturated films differs slightly from that used in Refs. 13 and 25.

[43]R. A. Ferrell, N. Menyhard, H. Schmidt, F. Schwabl, and P. Szepfalusy, Ann. Phys. (N.Y.) **47**, 565 (1968); B. I. Halperin and P. C. Hohenberg, Phys. Rev. **177**, 952 (1969); M. E. Fischer, M. N. Barber, and D. Jasnow, Phys. Rev. A **8**, 1111 (1973).

[44]P. W. Adams and W. I. Glaberson, Phys. Rev. Lett. **57**, 82 (1986); P. W. Adams, Ph.D. thesis, Rutgers University, 1986.

[45]M. Kim and W. I. Glaberson, Phys. Rev. Lett. **52**, 53 (1984).

[46]D. L. Huber, Phys. Lett. **79A**, 331 (1980).

[47]More power-law studies can be found in Ref. 25.

[48]D. H. Liebenberg, Phys. Rev. Lett. **29**, 794 (1971).

[49]B. Ratman and J. Mochel, Phys. Rev. Lett. **25**, 711 (1970).